Carcinogenesis vol.34 no.9 pp.2071–2079, 2013
doi:10.1093/carcin/bgt160
Advance Access publication May 13, 2013

MiR-146a enhances angiogenic activity of endothelial cells in hepatocellular carcinoma by promoting PDGFRA expression

Kai Zhu[1,2,†], Qi Pan[1,2,†], Xin Zhang[1,2,†], Ling-Qun Kong[1,2,†], Jia Fan[1,2], Zhi Dai[1,2], Lu Wang[1,2], Xin-Rong Yang[1,2], Jie Hu[1,2], Jin-Liang Wan[1,2], Yi-Ming Zhao[1,2], Zhong-Hua Tao[1,2], Zong-Tao Chai[1,2], Hai-Ying Zeng[3], Zhao-You Tang[1,2], Hui-Chuan Sun[1,2] and Jian Zhou[1,2,4,*]

[1]Liver Cancer Institute, Zhongshan Hospital, Fudan University, Shanghai 200032, China, [2]Key Laboratory of Carcinogenesis and Cancer Invasion, Fudan University, Ministry of Education, Shanghai 200032, China and [3]Department of Pathology and [4]Shanghai Key Laboratory of Organ Transplantation, Zhongshan Hospital, Fudan University, Shanghai 200032, China

*To whom correspondence should be addressed. Tel: +86 21 64041990; Fax: +86 21 64037181;
Email: zhou.jian@zs-hospital.sh.cn
Correspondence may also be addressed to Hui-Chuan Sun. Tel: +86 21 64041990; Fax: +86 21 64037181;
Email: sun.huichuan@zs-hospital.sh.cn

Endothelial cells (ECs) are critical for angiogenesis, and microRNAs play important roles in this process. We investigated the regulatory role of microRNAs in ECs of hepatocellular carcinoma (HCC) by examining the microRNA expression profile of human umbilical vein endothelial cells (HUVECs) in the absence or presence of human HCC cells, and identified miR-146a as the most highly upregulated microRNA. Furthermore, we revealed that miR-146a promoted the expression of platelet-derived growth factor receptor α (PDGFRA) in HUVECs, and this process was mediated by BRCA1. Overexpression of PDGFRA in the ECs of HCC tissues was associated with microvascular invasion and predicted a poorer prognosis. These results suggest that miR-146a plays a key role in regulating the angiogenic activity of ECs in HCC through miR-146a–BRCA1–PDGFRA pathway. MiR-146a and PDGFRA may emerge as potential anti-angiogenic targets on ECs for HCC therapy.

Introduction

Angiogenesis is a fundamental hallmark of cancer and is critical to the multistep progression of cancer (1,2). Endothelial cells (ECs) play a key role in this process by proliferating, migrating and lining the lumen of blood vessels (1). A better understanding of the mechanisms underlying the angiogenic activity of ECs may help us develop new strategies for targeting tumor vessels.

Increasing evidence has indicated that microRNAs are important in multiple physiological and pathological processes, including carcinogenesis and metastasis (3,4). MicroRNAs are small non-coding RNAs composed of 20–22 nucleotides that can inhibit protein expression by binding to the 3′ untranslated region (UTR) of target messenger RNA (mRNA), which results in transcriptional repression or degradation of target mRNA (5).

MicroRNAs have recently been shown to regulate EC activity and angiogenesis (6), several approaches have been utilized to investigate the regulatory mechanism. For instance, some researchers explored the role of microRNAs in ECs by specifically silencing Dicer and Drosha, which are required for angiogenesis, and found that several candidate microRNAs were involved in endothelial processes (7–9). Other EC-specific microRNAs have also been identified by exposing ECs to tumor cells (10) or hypoxia (11). Nonetheless, the consequences of microRNA activity on tumor-associated ECs in tumor tissues remain unclear. This study explores the role of microRNAs in the angiogenic activity of ECs in hepatocellular carcinoma (HCC) tissues.

Abbreviations: ChIP, chromatin immunoprecipitation; ECs, endothelial cells; HCC, hepatocellular carcinoma; HUVECs, human umbilical vein endothelial cells; mRNA, messenger RNA; PDGFRA, platelet-derived growth factor receptor α; siRNAs, small interfering RNAs; UTR, untranslated region; wt, wild-type.

[†]These authors contributed equally to this work.

Materials and methods

Cells and animals

The HCC cell line HCCLM3 was used in this study and was maintained in Dulbecco's modified Eagle's medium (GIBCO 11995; Invitrogen, Carlsbad, CA). Human umbilical vein endothelial cells (HUVECs) (8000; Sciencell, Carlsbad, CA) were maintained in EGM-2 medium (CC-4147; Lonza, Basel, Switzerland), and only passages 3–7 were used. For co-culturing, six-well transwell permeable supports (3414; Corning Inc., Corning, NY) containing 3 μm pores in the inserts were used; they allowed diffusible molecules, but not cells, to pass through. The HUVECs were plated onto the inserts, and the HCC cells were plated onto the chambers at a HUVEC:HCCLM3 cell ratio of 1:5 (Supplementary Figure S1A, available at *Carcinogenesis* Online). After 24 h, the HUVECs were collected for further investigation. Male athymic BALB/c nude mice were purchased from Shanghai Institute of Material Medicine, Chinese Academy of Science, and were raised in specific pathogen-free conditions. Animal care and experimental protocols were conducted in accordance with guidelines established by the Shanghai Medical Experimental Animal Care Commission.

Genome-wide microRNA analysis

The microRNA expression profile of HUVECs was determined using the Agilent-025218 Human MicroRNA Array Kit (V3) (G4470C; Agilent Technologies, Santa Clara, CA), which contains probes for 866 human and 89 viral microRNAs from the Sanger database (version 12.0) (http://www.chem.agilent.com/en-US/Store/_layouts/Agilent/Commerce/ProductDetail.aspx?productID=G4470C&cat=miRNA&pcat=DNAMicroarraysSub&rcat=DNAMicroarrays). Four replicates were used in each group. The assay and data analyses were performed at Shanghai Biochip Company according to the protocols of the Agilent microRNA microarray system (12); briefly, expression levels of 866 human and 89 viral microRNAs in the co-cultured samples ($n = 4$) and control samples ($n = 4$) were compared by independent-samples t-test and a two-tailed value of $P < 0.05$ was used to indicate a significant result.

Gene expression analysis of HUVECs and miR-146a overexpressing HUVECs was performed using the Human OneArray (Phalanx Biotech Group) as described previously (13). The log2-transformed expression ratio (miR-146a overexpressing clones versus control clones) of each gene was calculated. The probes with log2 ratio ≥ 1 or log2 ratio ≤ −1 and P-value < 0.05 were defined as differential genes. For further pathway enrichment analysis of angiogenesis, please see Supplementary file.xls, available at *Carcinogenesis* Online.

Cell transfection and clone selection

MicroRNAs upregulation and downregulation were achieved by using a lentivector-mediated pseudoviral system (LV500A-1; System Biosciences, San Francisco, CA). For permanent inhibition of miR-146a, vectors bearing an anti-146a sequence (MZIP146a-PA-1; System Biosciences) were packaged into the virus. To obtain stable miR-146a overexpressing cells, HUVECs were infected with viruses carrying a miR-146a precursor (pre-146a) sequence (PMIRH146aPA-1; System Biosciences). The procedure was performed according to the manufacturer's instructions. Infected cells expressed green fluorescent protein and the efficiency of the procedure was determined by the intensity of the fluorescence (Supplementary Figure S1B, available at *Carcinogenesis* Online). For the inhibition of BRCA1 or platelet-derived growth factor receptor α (PDGFRA), the transfection of small interfering RNAs (siRNAs) targeting the mRNA (Supplementary Table S1, available at *Carcinogenesis* Online) was performed using Lipofectamine 2000 (GIBCO-11668-027; Invitrogen) according to the manufacturer's instructions.

To overexpress PDGFRA, a lentiviral expression system (Addgene) was used. The open reading frame of PDGFRA (Supplementary Table S1, available at *Carcinogenesis* Online) was inserted into pWPXL vectors between the

XhoI and SalI sites. The pWPXL vectors, the packaging plasmid psPAX2 and the envelope plasmid pMD2.G were co-transfected into 293T cells using Lipofectamine 2000 reagent (Life Technologies). The virus particles were then harvested 48 h after transfection. The HUVECs were infected at a multiplicity of infection of 10 with 5 μg/ml polybrene (Sigma–Aldrich).

Cell proliferation assay

For proliferation assays, Cell-IQ system (Chip-man Technologies, Tampere, Finland), which can capture images of cells at regular intervals, was used. The assay was performed according to the manufacturer's instructions. Cells were cultured in a 24-well plate at a density of approximately 2.5×10^4 cells per well. The plate was then placed in the Cell-IQ system and monitored for 4 days. For cell proliferation, the total cell number was analyzed every 8 h with the Cell-IQ Analyzer Pro-Write V.AN 2.3.0 (Chip-man Technologies) using continuous images. Four replicates were used in each group.

Scratch, two-chamber migration and tube formation assays

Scratch and two-chamber migration assays were performed as described previously (14). For the tube formation assay, a 96-well plate was coated with 50 μl Matrigel (356234; BD Bioscience, Franklin Lakes, NJ) per well according to the manufacturer's instructions. HUVECs (15 000 cells in 100 μl) were seeded on the gel for 4 h at 37°C and tube formation was imaged under a microscope. Tube formation ability was assessed by counting the number of branches per field. Four replicates were used in each group.

Ectopic transplants and immunohistochemistry

About 1×10^6 HCCLM3 cells in combination with 1×10^7 HUVECs were suspended in phosphate-buffered saline and injected subcutaneously into the right front flanks of the nude mice. The HUVECs were infected with lentivirus and expressed either high or low levels of miR-146a. After 4 weeks, the mice were killed and tumor volumes were measured as described previously (length × width$^2\pi/6$) (15). Paraffin-embedded sections were made from the tumors. Protocols for immunohistochemistry were described previously (16). Images were obtained using a microscope (BX51; Olympus, Tokyo, Japan). The microvessel density was evaluated as described (17), and the mean microvessel count of five fields was taken as the microvessel density, which was expressed as the absolute number of microvessels per 0.74 mm^2 (×200 field).

Tissue microarray and ECs isolation

A tissue microarray of 323 HCC patients was used to assess the expression of PDGFRA and its prognostic significance. All of the patients underwent curative liver resection for primary tumors. The inclusion criteria of the patient and the follow-up procedures were carried out as described previously (14). The intensity of PDGFRA staining was divided into high and low group (14).

For ECs isolation, fresh tumor and corresponding normal liver tissues (at least 2 cm from the margin of the tumor) were obtained from 20 patients who had received curative resection for HCC in our hospital. None of these patients received any preoperative anticancer treatment including chemotherapy or anti-angiogenesis drugs. The study was approved by the Zhongshan Hospital Research Ethics Committee and informed consent was obtained according to the committee's regulations. Cell suspension of tumor or corresponding normal liver tissue was prepared as described previously (18). Isolation of ECs from the cell suspension was performed using anti-CD31 antibody coupled to magnetic beads (130-091-935; Miltenyi Biotech, Bergisch Gladbach, Germany) and magnetic cell-sorting using the MACS system (Miltenyi Biotech). To increase the purity of isolated ECs, the cell pellets underwent a second isolation with anti-CD31 beads.

Real-time PCR and western blot

Total RNA was isolated using Trizol reagent (15596-026; Invitrogen). For microRNA, total RNA was reverse transcribed to complementary DNA using a MicroRNA Reverse Transcription Kit (TaqMan®, 4366596; Applied Biosystems, Carlsbad, CA) and real-time PCR (RT–PCR) was performed using Universal PCR Master Mix (TaqMan®, 4324018; Applied Biosystems) according to the manufacturer's instructions. U6 small nuclear RNA was used as the internal control. For mRNA, the procedure was described previously (14). Western blots were performed as described previously (19). The images were captured through Gel Doc XR system (Bio-Rad, Philadelphia, PA) and analyzed using Image Lab™ software (version 2.0). The antibodies are listed in Supplementary Table S1, available at *Carcinogenesis* Online.

MicroRNA target reporter assay

Wild-type-UTR (wt-UTR) (forward: 5′-GGACTAGTGTCCTTCTACTGTCCTGGCTAC-3′, reverse: 5′-CGACGCGTCCTCCCCAATGTTCCAC-3′) and mutant-UTR (forward: 5′-GGACTAGTCCACAGGACCCCAAGAATG-3′, reverse: 5′-CGACGCGTGCGACATGCCCAAGGACTATTCTGACTTTAAG-3′) of BRCA1 mRNA were cloned into the pMIR-REPORT™ microRNA Expression Reporter Vector System (AM5795; Applied Biosystems); they were then transfected into 293T cells. The 293T cells were also transfected with vectors containing pre-146a, anti-146a or their controls as mentioned in the Cell transfection and clone selection. After 24 and 48 h, cells were lysed and luciferase activity was measured using Dual-Luciferase Reporter Assay System (E1910; Promega, Madison, WI).

Luciferase reporter gene assay

Luciferase reporter gene assay was carried out as described previously (20). pGL3 plasmid (E1761; Promega) with luciferase reporter gene was used. 293T cells were transfected with pGL3 plasmid containing full-length PDGFRA promoter. The luciferase assay was performed according to the manufacturer's protocol.

Chromatin immunoprecipitations

Chromatin immunoprecipitation (ChIP) assay was performed using SimpleChIP Enzymatic Chromatin IP Kit (Agarose Beads) according to the manufacturer's instructions. The antibody used for immunoprecipitation of BRCA1 was purchased from Cell signaling (9010).

Statistical analysis

Statistical analyses were performed with SPSS 17.0 software (SPSS, Chicago, IL) as described previously (14). Two-tailed value of $P < 0.05$ was used to indicate a significant result.

Results

HCCLM3 increases pro-angiogenic capacity and miR-146a expression of HUVECs

To explore the effect of HCC cells on ECs, we co-cultured a human HCC cell line with a high metastatic potential (HCCLM3) and HUVECs to simulate the interaction of HCC cells with ECs. Six-well transwell permeable supports were used, with 3 μm pores in the inserts, which allowed soluble molecules to pass through while keeping the two cell lines separated. The HUVECs were plated onto the inserts and HCC cells were plated onto the chambers at a HUVEC:HCCLM3 cell ratio of 1:5. The HUVECs cultured alone served as the control. In this co-culturing system, the HUVECs proliferate, migrate and form tubule-like sprouts that mimic the development of microvessels *in vivo* (21). The HUVECs co-cultured with HCCLM3 cells grew more rapidly than the HUVECs cultured alone, as determined by a cell proliferation assay (Figure 1A), indicating that HCCLM3 cells may promote the proliferation of HUVECs. In addition, HCCLM3 cells promoted the migratory ability of HUVECs, as shown by scratch (Figure 1B and C) and two-chamber migration assays (Figure 1D and E). The HUVECs exposed to HCCLM3 cells also formed more branches in the tube formation assay (Figure 1F and G). These results suggest that HCCLM3 cells may enhance the angiogenic activity of HUVECs.

After 24 h of culturing, the HUVECs were harvested. MicroRNAs were then extracted from the HUVECs and tested using a MicroRNA Microarray Kit containing probes for 866 human and 89 viral microRNAs (http://www.ncbi.nlm.nih.gov/geo/query/acc.cgi?acc=GSE44567). Twelve microRNAs from the co-cultured HUVECs were differentially expressed ($P < 0.05$) (Supplementary Table S2, available at *Carcinogenesis* Online), of which miR-146a was the most highly upregulated microRNA. The results were then validated by applying RT–PCR to the 12 dysregulated microRNAs. Thus, we narrowed our lists to four microRNAs that either increased or decreased by at least 1.5 times (miR-146a, miR-302c, miR-181a* and miR-140-5p) (Supplementary Figure S1C, available at *Carcinogenesis* Online). Among these four microRNAs, miR-146a was still the most remarkable upregulated microRNA. Therefore, we chose miR-146a for further investigation.

MiR-146a enhances the angiogenic activities of ECs

To further investigate the role of miR-146a in angiogenesis, we created HUVEC cell lines with either increased (pre-146a) or reduced (anti-146a) expression of miR-146a using a lentivector-mediated pseudoviral system. The transduction efficiencies were confirmed by RT–PCR (Figure 2A). Consistent with the results observed in co-cultured HUVECs, forced expression of miR-146a in HUVECs led to an increased proliferation rate (Figure 2B), enhanced migratory (Figure 2C–F) and tube forming abilities (Figure 2G and H). In contrast, the knockout of miR-146a impaired these abilities.

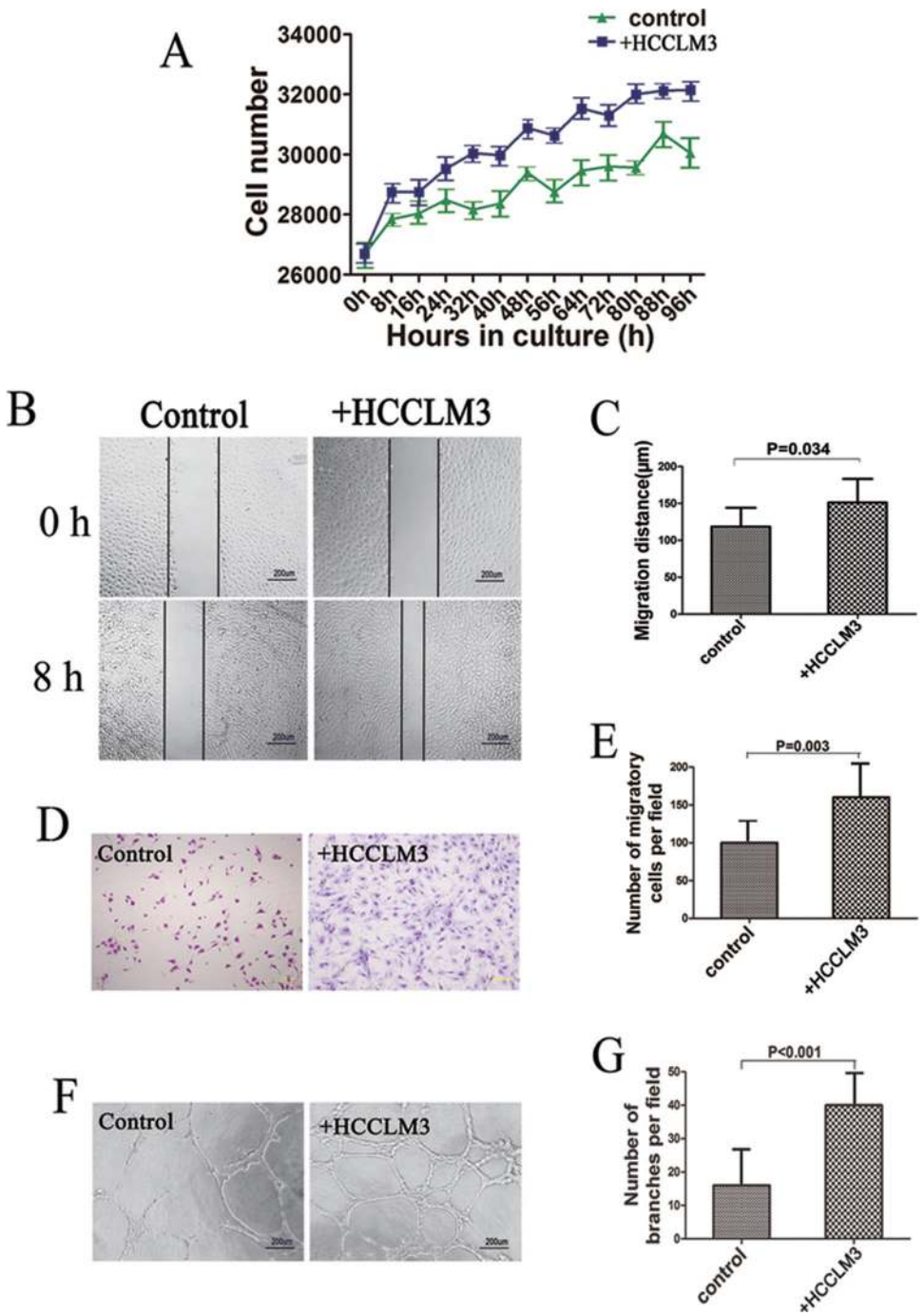

Fig. 1. Phenotypic changes of HUVECs exposed to different conditions. (**A**) Growth curves of HUVECs cultured alone or with HCCLM3 cells in a 24-well plate. (**B**) Representative images of scratch assay in HUVECs. (**C**) Quantification of migration distances shown in B. (**D**) Images of two-chamber migration assay. (**E**) Quantification of the number of migratory cells shown in D. (**F**) Images of tube formation assay. (**G**) Quantification of the number of branches in tube formation shown in F.

To test whether miR-146a contributes to the angiogenesis of ECs *in vivo*, we co-injected HCCLM3 cells and HUVECs (harboring either gain or loss of miR-146a) in the right flanks of the nude mice. After 4 weeks, all groups formed tumors in the flanks. The upregulation of miR-146a in HUVECs resulted in an almost 2-fold increase in tumor volume compared with the control group and the downregulation of miR-146a resulted in a reduction in tumor volume as well (Figure 3A and C). Then, we focused on the blood vessels formed by HUVECs in the tumors. Forced expression of miR-146a in HUVECs led to more HUVEC-origin vessels, whereas inhibition of miR-146a led to fewer vessels (Figure 3B and D). These results validate the role of miR-146a in regulating angiogenic abilities of ECs *in vivo*.

MiR-146a promotes angiogenic activity of ECs through PDGFRA overexpression

To investigate the potential mechanism of miR-146a-induced angiogenesis, we performed a microarray assay to compare the differential gene expression profiles between miR-146a overexpressing HUVECs and control HUVECs (http://www.ncbi.nlm.nih.gov/geo/query/acc.cgi?acc=GSE46022). About 2497 genes were differentially expressed, of which, 1626 genes were upregulated, and 871

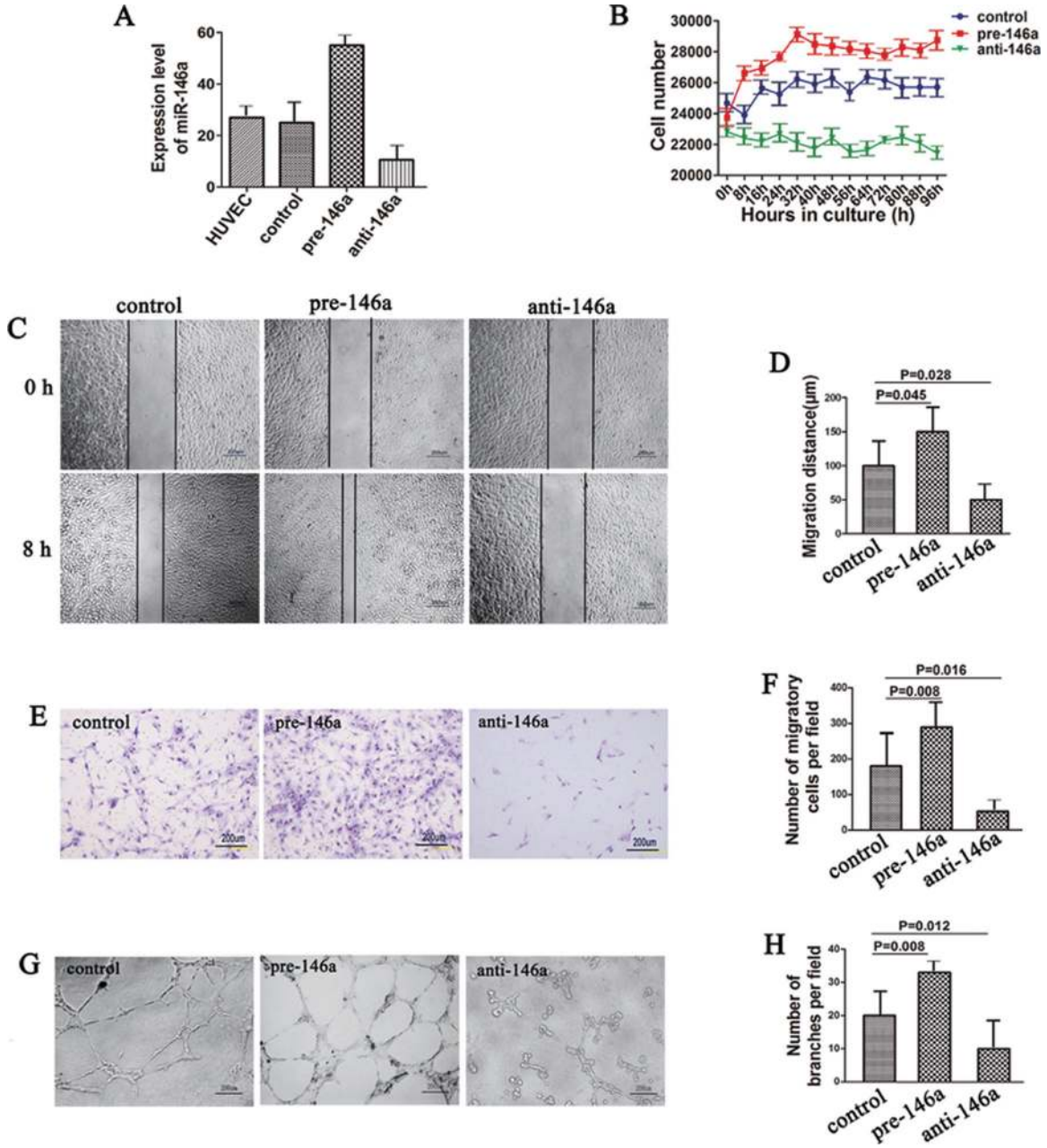

Fig. 2. Effect of miR-146a on proliferation, migration and tube formation of HUVECs. (**A**) Transduction efficiency of lentivirus containing pre-146a or anti-146a assessed by RT–PCR; U6 was used as internal control; (control versus pre-146a, $P < 0.05$; control versus anti-146a, $P < 0.05$). (**B**) Growth curves of HUVECs harboring either gain or loss of miR-146a cultured in a 24-well plate. (**C**) Representative images of scratch assay in HUVECs with different levels of miR-146a. (**D**) Quantification of migration distances shown in C. (**E**) Images of two-chamber migration assay. (**F**) Quantification of the number of migratory cells shown in E. (**G**) Images of tube formation assay. (**H**) Quantification of the number of branches in tube formation shown in G.

genes were downregulated. Further pathway enrichment analysis for angiogenesis showed that 54 genes were closely related to angiogenesis, of which, 31 genes were upregulated, and 23 genes were downregulated (Supplementary file.xls, available at *Carcinogenesis* Online).

A hallmark of pathological angiogenesis is the high expression of pro-angiogenic growth factor receptors in proliferating ECs, such as PDGFR (10). Among the differentially expressed genes, there are three growth factor receptors (PDGFRA, VEGFR-1 and VEGFR-2). Therefore, we analyzed the effect of miR-146a on these receptors by RT–PCR and western blot analyses. The results showed that after miR-146a was overexpressed in HUVECs, a significant increase was observed in PDGFRA expression (Figure 3E and Supplementary Figure S1D, available at *Carcinogenesis* Online).

To explore the function of PDGFRA in the angiogenic activity of ECs, we transiently inhibited PDGFRA expression in HUVECs by siRNA (Figure 4A). The inhibition of PDGFRA resulted in decreased cell proliferation rate (Figure 4B). We also tested the role of PDGFRA in the migration and tube formation of HUVECs. The inhibition of PDGFRA in HUVECs resulted in a reduction of migratory ability (Figure 4C–F) and a decrease in the number of branches in the tube formation assay (Figure 4G and H). On the other hand, when PDGFRA was overexpressed through a lentiviral expression system (Figure 4A), the opposite results were observed in HUVECs (Figure 4B–H).

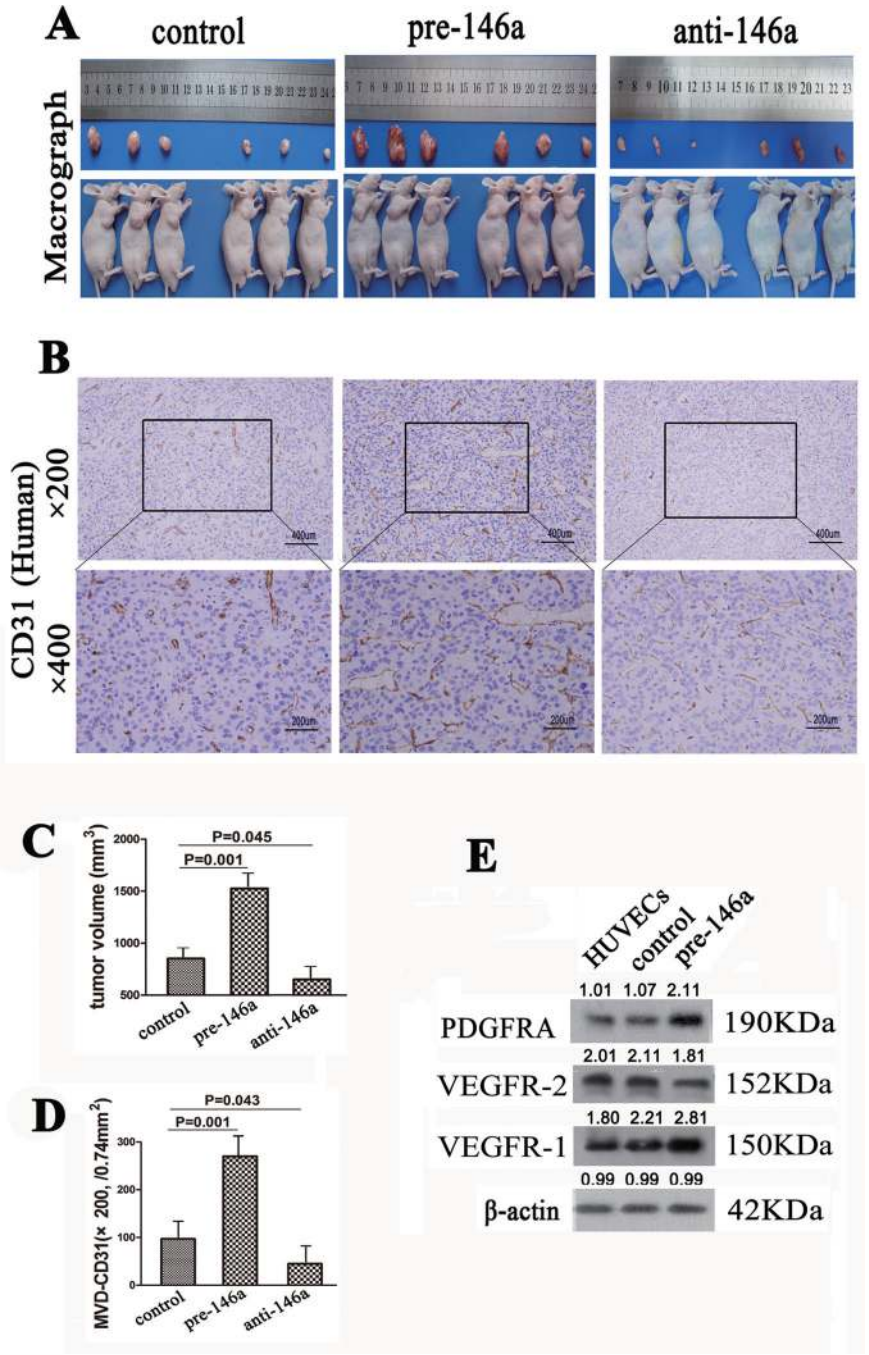

Fig. 3. Role of miR-146a in regulating angiogenesis. (**A**) Macroscopic tumors formed by injecting HCCLM3 cells and HUVECs in the right flanks of the nude mice. (**B**) Images of HUVEC-related neoangiogenesis assessed by immunostaining of CD31 (human). (**C**) Quantification of the tumor volume. (**D**) Quantification of the number of vessels per field (×200). (**E**) Western blot results of expression of growth factor receptors in HUVECs transfected with pre-146a.

To assess the clinical relevance of PDGFRA in HCC patients, we measured its expression in a tissue microarray of 323 HCC patients. The results showed that HCC tumor cells were negative for PDGFRA staining, and its staining was mainly observed in small vessels (Figure 5A). The density of PDGFRA-positive staining was consistent with microvascular invasion (Supplementary Table S3, available at *Carcinogenesis* Online), which means that HCC tumors with more PDGFRA-positive ECs are prone to bear microvascular invasion. We then analyzed the correlation between PDGFRA staining and the patients' outcome. Patients in PDGFRA high group tended to suffer more recurrence and have a shorter overall survival (Figure 5B).

MiR-146a promotes PDGFRA expression through suppression of BRCA1

Our data revealed that miR-146a can promote PDGFRA expression. Because microRNAs usually inhibit protein expression by degrading its mRNA (5), we assume that some other protein may mediate the regulation of PDGFRA by miR-146a.

To further investigate how miR-146a promotes PDGFRA expression, we made bioinformatic prediction of potential target genes of miR-146a using the microRNA target predicting program miRanda (http://www.microrna.org/microrna/searchGenes.do). Among the predicted targets, BRCA1 was one of the highest scoring target genes, with a miR-146a binding site in the 3′UTR of its mRNA (Supplementary

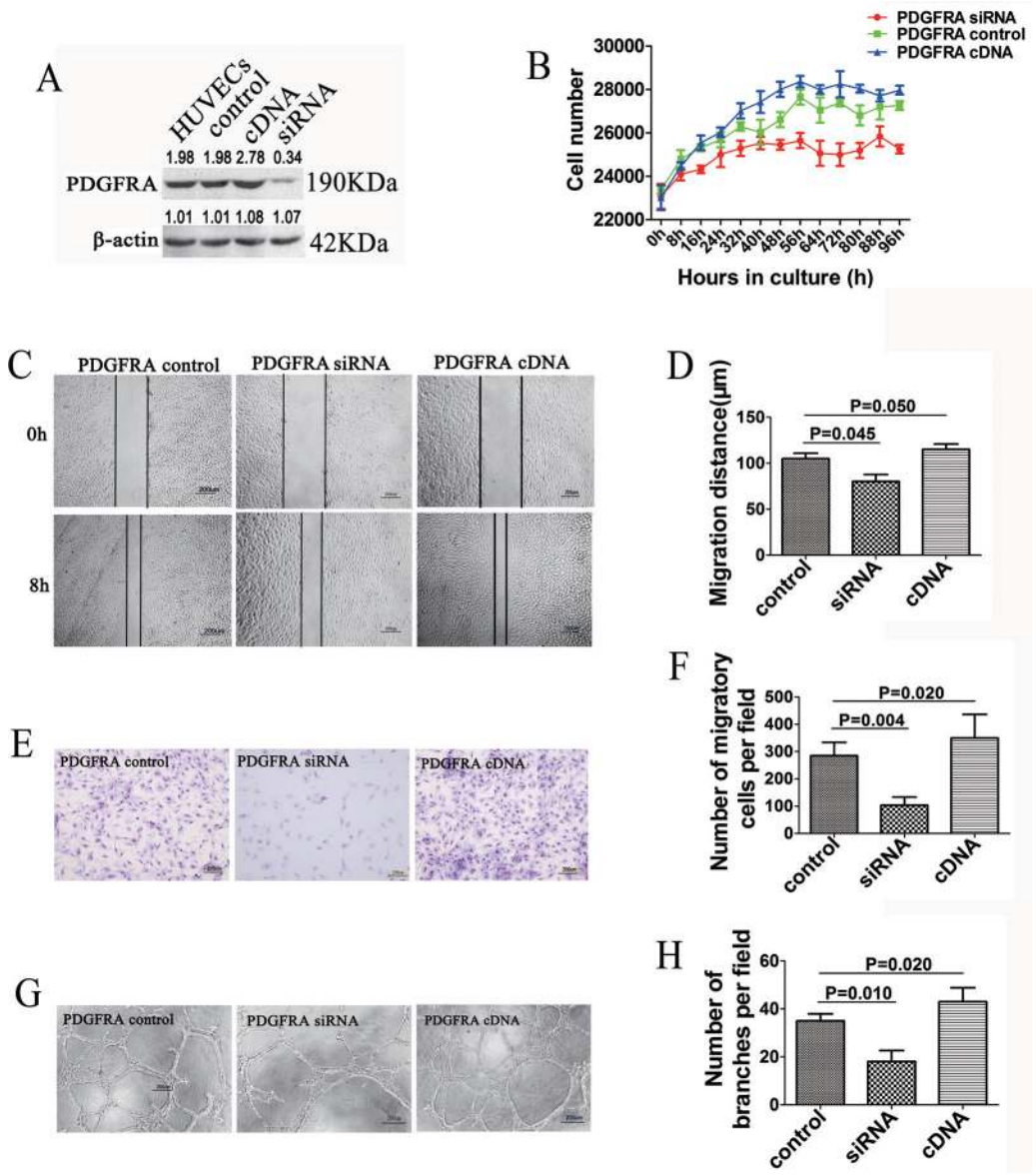

Fig. 4. Effect of PDGFRA on HUVECs. (**A**) Transduction efficiency of PDGFRA complementary DNA and siRNA in HUVECs confirmed by western blot analysis. (**B**) Growth curves of HUVECs with different levels of PDGFRA, cultured in a 24-well plate. (**C**) Images of scratch assay in HUVECs. (**D**) Quantification of migration distances shown in C. (**E**) Images of two-chamber migration assay. (**F**) Quantification of the number of migratory cells shown in E. (**G**) Images of tube formation assay. (**H**) Quantification of the number of branches in tube formation shown in G.

Figure S2A, available at *Carcinogenesis* Online). In addition, BRCA1 has been found to be associated with neovascularization (20,22). Therefore, we hypothesized that miR-146a may promote PDGFRA expression by the transcriptional inhibition of BRCA1.

RT–PCR and western blot analysis revealed that the upregulation of miR-146a led to the downregulation of BRCA1 in HUVECs (Supplementary Figure S1D and S2B, available at *Carcinogenesis* Online). To test whether miR-146a inhibits BRCA1 by directly binding to the 3′UTR of its mRNA, we performed reporter assays with a luciferase vector containing either the wt- or mutant-UTR of BRCA1 mRNA (Supplementary Figure S2A, available at *Carcinogenesis* Online). The results showed that the upregulation of miR-146a reduced the luciferase activity of wt-UTR, whereas the inhibition of miR-146a resulted in a significant increase of luciferase activity. However, when the binding site of miR-146a in BRCA1 mRNA was mutated, the luciferase activity did not change under miR-146a regulation (Figure 6A). These results suggest that miR-146a inhibits BRCA1 expression by directly binding to its 3′UTR thereby degrading its mRNA.

Then, we tried to explore the relationship between BRCA1 and PDGFRA. Western blot analysis showed that PDGFRA expression was markedly upregulated when BRCA1 expression was knocked-down by BRCA1-siRNA; and its expression did not change when anti-146a was added to inhibit miR-146a level (Figure 6B). These results further confirm that BRCA1 mediates the regulation of PDGFRA by miR-146a.

BRCA1 is a nuclear phosphoprotein, which can combine with other tumor suppressors, DNA damage sensors and signal transducers to form a large multisubunit protein complex known as the BRCA1-associated genome surveillance complex, thus playing a role in transcription, DNA repair of double-stranded breaks and recombination (20). We assume that BRCA1 may confer a transcriptional repression on PDGFRA *via* binding to its promoter. Luciferase reporter gene assay showed that when BRCA1 was inhibited, the luciferase activity of PDGFRA promoter increased significantly (Figure 6C). Then, we tried to determine whether BRCA1 is bound to specific sequences in PDGFRA promoter.

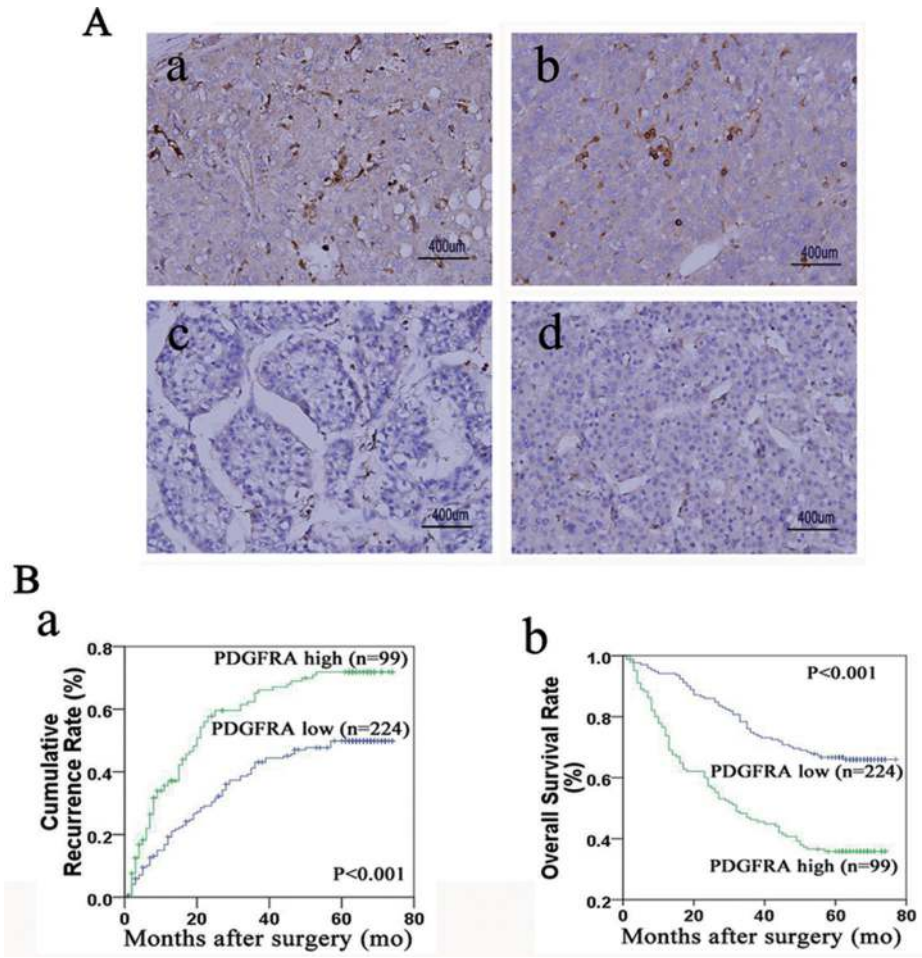

Fig. 5. Expression of PDGFRA in HCC and its prognostic significance. (**A**) Staining of PDGFRA in the tissue microarray of 323 HCC patients. (a) and (b), high PDGFRA staining; (c) and (d), low PDGFRA staining. (**B**) Prognostic significance of PDGFRA assessed by Kaplan–Meier analysis and log-rank tests. Overexpression of PDGFRA predicts higher cumulative recurrence rate (a) and lower overall survival rate (b).

ChIP analysis confirmed that there are three BRCA1-binding sites in PDGFRA promoter (1901–2000, 1601–1700 and 901–1000, respectively) (Figure 6D and E).

We then examined the relative levels of miR-146a, BRCA1 and PDGFRA in ECs isolated from tumors and corresponding normal liver tissues of 20 HCC patients. All of the patients underwent curative liver resection for primary HCC and had not received anticancer treatment before resection. The blood vessels in tumor tissues were more tortuous and dilated than in normal liver tissues (Supplementary Figure S2C, available at *Carcinogenesis* Online). RT–PCR results showed that ECs isolated from tumor tissues expressed significantly higher levels of miR-146a and PDGFRA, but a lower level of BRCA1 than those isolated from normal liver tissues (Supplementary Figure S2D, available at *Carcinogenesis* Online). Similar results were seen in HUVEC-origin ECs isolated from xenografts that overexpression of miR-146a led to higher level of PDGFRA, but lower level of BRCA1 and *vice versa* (Supplementary Figure S2E, available at *Carcinogenesis* Online). We also observed that the tumors with high levels of miR-146a in ECs tended to contain more blood vessels, which were more tortuous and dilated than those with low levels of miR-146a in ECs (Supplementary Figure S2F, available at *Carcinogenesis* Online).

Discussion

HCC is a highly angiogenic malignancy, which is characterized by a high propensity for vascular invasion. ECs can respond to stimulation from tumor cells by transforming into an 'activated phenotype' with increased proliferation, migration and tube formation, and form the lumen of blood vessels, and thereby play a critical part in tumor angiogenesis, invasion and metastasis (18). This activated phenotype of ECs was also observed in this study when they are exposed to HCC cells with high potential of invasion and metastasis.

Recent reports suggested that microRNAs might be involved in the regulation of tumor angiogenesis (6,10). These microRNAs belong to a new family of 'angiomirs' (10), which are functionally linked to the angiogenic phenotype. However, the effect of microRNAs in ECs responding to stimulation of tumor cells is not clear. We, therefore, analyzed the microRNA expression profile of ECs in the absence or presence of HCC cells. In the array result, there were only 12 differentially expressed microRNAs, among which four microRNAs either increased or decreased by >1.5 times.

We chose the most highly upregulated microRNA, miR-146a, for further investigation. Previous studies have demonstrated the importance of miR-146a in multiple physiological and pathological conditions (23). MiR-146a can regulate the innate immune system, inflammatory responses and antiviral pathways (24). It also plays a role in several human diseases such as cancer (25–28). For instance, the overexpression of miR-146a was observed in papillary thyroid carcinoma and was associated with loss of KIT transcript and Kit protein (25); miR-146a was also found to promote cell proliferation in cervical cancer (29). However, the role of miR-146a in regulating the angiogenic activity of tumor-associated ECs has never been investigated. Using a series of *in vitro* and *in vivo* experiments, we were able to show that the upregulation of miR-146a in HUVECs increased

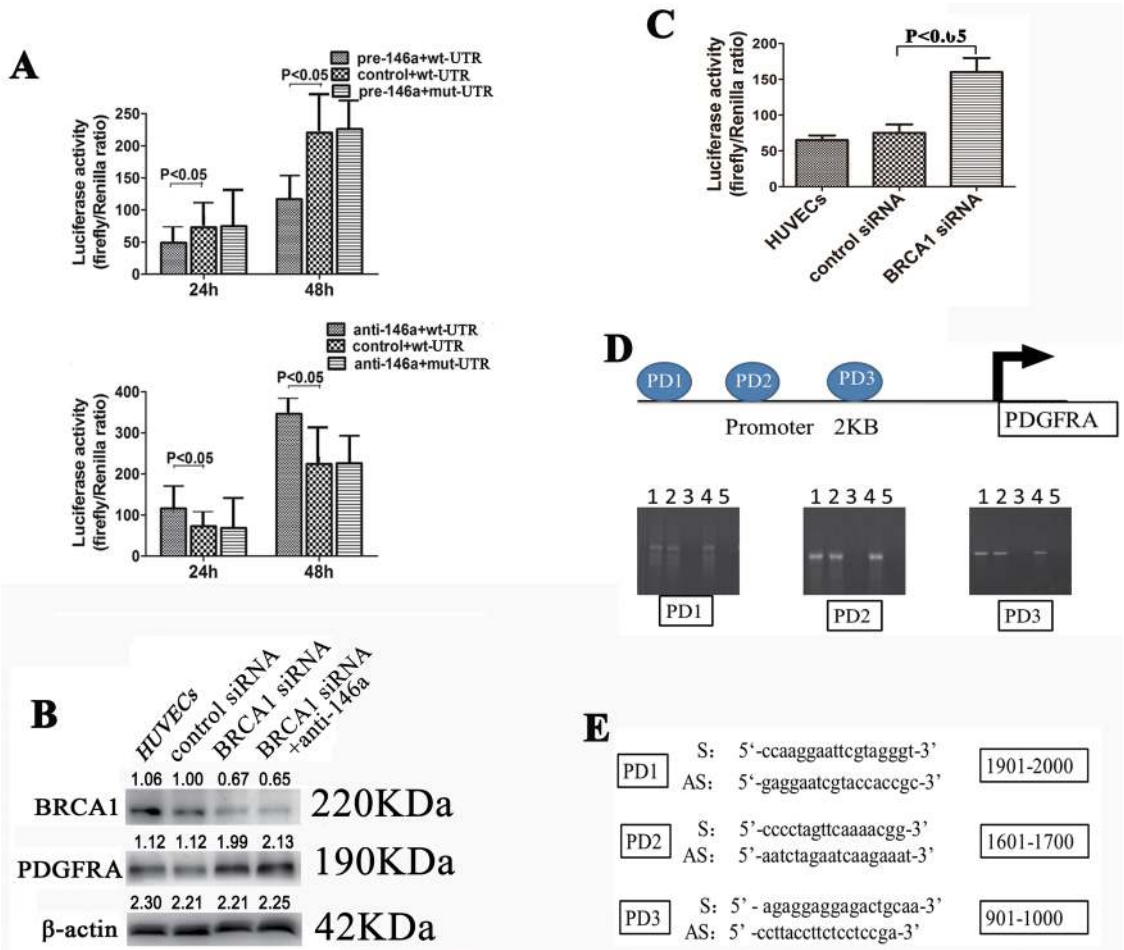

Fig. 6. Relationships between miR-146a, BRCA1 and PDGFRA. (**A**) Reporter gene analysis of miR-146a on 3′UTR of wt- and mutant-BRCA1 mRNA. (**B**) Western blot results of PDGFRA in HUVECs transfected with siRNAs targeting BRCA1 mRNA and anti-146a. (**C**) Reporter gene analysis of BRCA1 on PDGFRA promoter. (**D**) BRCA1 binds to PDGFRA promoter at three sites. ChIP assays were done in 293T cells. Lanes 1 and 2, input; lane 3, IgG; lane 4, BRCA1 antibody; lane 5, no antibody. (**E**) The three binding sites of BRCA1 at PDGFRA promoter, and the primers used for amplification of the fragments.

their abilities of proliferation, migration and tube formation, whereas downregulation of miR-146a decreased these abilities. These results suggest that miR-146a plays a key role in regulating angiogenic activity of ECs in HCC.

Because microRNAs can potentially modulate multiple downstream proteins (30), and the same microRNA may regulate different cells through various mechanisms due to their diverse cell types and microenvironment, it is necessary to identify the specific signaling pathway in miR-146a-mediated EC activation in HCC. By comparing the differential gene expression profiles between miR-146a overexpressing HUVECs and control HUVECs, we revealed that PDGFRA had a positive correlation with miR-146a. Our previous study already showed that the gene expression of HCC vascular endothelium was different between tumors with different metastatic potential, and PDGFRA was overexpressed in endothelium of highly metastatic HCC, as compared with that of low metastatic HCC (31). By a series of *in vitro* experiments, our results also proved the regulatory role of PDGFRA in EC activities. We further investigated its clinical significance by measuring its expression in the tumor tissue of 323 HCC patients, which reveals that PDGFRA overexpression predicts a shorter overall survival and higher recurrence rate in HCC patients, suggesting that it may serve as a candidate biomarker for prognosis of HCC patients. Nevertheless, the manner in which PDGFRA regulates EC activity requires further investigation.

In this study, we identified for the first time the regulation of HCC angiogenesis by the miR-146a–BRCA1–PDGFRA pathway. First, using microRNA target reporter assay, we showed that miR-146a inhibits BRCA1 expression by directly binding to its 3′UTR and thereby degrading BRCA1 mRNA. Second, luciferase reporter gene assay revealed that BRCA1 can suppress the activity of PDGFRA promoter; besides, we performed ChIP assay to prove that BRCA1 has a direct contact with PDGFRA promoter, and thus inhibits PDGFRA expression. Third, when BRCA1 is suppressed, miR-146a loses its effect on PDGFRA expression. Furthermore, we detected an increase of miR-146a and PDGFRA, as well as a decrease of BRCA1 in ECs isolated from HCC tissues, as compared with those from corresponding normal liver tissues. Thus, our results suggest that miR-146a plays a key role in regulating the angiogenic activity of ECs in HCC through miR-146a–BRCA1–PDGFRA pathway.

In this study, HUVECs and HCC cells were co-cultured using transwell supports, so they did not have direct contact. As a result, the HUVECs may be activated by soluble factors released by HCC cells. Because HCC cells can secrete a large number of soluble factors, which factors are responsible for the activation of HUVECs will be the next phase of our study. Due to difficulties in collecting a sufficient quantity of ECs from HCC tumors for the assay, we only obtained 20 HCC-associated EC samples. Nevertheless, to our knowledge, this is the first study that explores the role of miR-146a in regulating HCC-associated angiogenesis.

In conclusion, this study demonstrates that miR-146a promotes the angiogenic activity of HCC-associated ECs through miR-146a–BRCA1–PDGFRA pathway. Our results suggest that miR-146a may emerge as a potential anti-angiogenic target for HCC therapy.

Supplementary material

Supplementary Tables S1–S3, Figures S1 and S2 and files.xls can be found at http://carcin.oxfordjournals.org/

Funding

National Key Sci-Tech Special Project of China (2012ZX10002-016); National Science Fund for Distinguished Young Scholars of China (81225019); National Natural Science Funds of China (30801102); Shanghai Key-Tech Research and Development Program (09411951700).

Conflict of Interest Statement: None declared.

References

1. Kerbel,R.S. (2008) Tumor angiogenesis. *N. Engl. J. Med*., **358**, 2039–2049.
2. George,A.L. *et al.* (2011) Endothelial progenitor cell biology in disease and tissue regeneration. *J. Hematol. Oncol*., **4**, 24.
3. Budhu,A. *et al.* (2010) The clinical potential of microRNAs. *J. Hematol. Oncol*., **3**, 37.
4. Zhang,H. *et al.* (2011) Genome-wide functional screening of miR-23b as a pleiotropic modulator suppressing cancer metastasis. *Nat. Commun*., **2**, 554.
5. Calin,G.A. *et al.* (2006) MicroRNA signatures in human cancers. *Nat. Rev. Cancer*, **6**, 857–866.
6. Wang,S. *et al.* (2009) AngiomiRs–key regulators of angiogenesis. *Curr. Opin. Genet. Dev.*, **19**, 205–211.
7. Kuehbacher,A. *et al.* (2007) Role of Dicer and Drosha for endothelial microRNA expression and angiogenesis. *Circ. Res*., **101**, 59–68.
8. Suárez,Y. *et al.* (2007) Dicer dependent microRNAs regulate gene expression and functions in human endothelial cells. *Circ. Res*., **100**, 1164–1173.
9. Suárez,Y. *et al.* (2008) Dicer-dependent endothelial microRNAs are necessary for postnatal angiogenesis. *Proc. Natl Acad. Sci. USA*, **105**, 14082–14087.
10. Würdinger,T. *et al.* (2008) miR-296 regulates growth factor receptor overexpression in angiogenic endothelial cells. *Cancer Cell*, **14**, 382–393.
11. Fasanaro,P. *et al.* (2008) MicroRNA-210 modulates endothelial cell response to hypoxia and inhibits the receptor tyrosine kinase ligand Ephrin-A3. *J. Biol. Chem*., **283**, 15878–15883.
12. Wang,S. *et al.* (2010) Improvement of tissue preparation for laser capture microdissection: application for cell type-specific miRNA expression profiling in colorectal tumors. *BMC Genomics*, **11**, 163.
13. Qu,Y. *et al.* (2011) Thioredoxin-like 2 regulates human cancer cell growth and metastasis via redox homeostasis and NF-κB signaling. *J. Clin. Invest*., **121**, 212–225.
14. Zhu,K. *et al.* (2011) Metadherin promotes hepatocellular carcinoma metastasis through induction of epithelial-mesenchymal transition. *Clin. Cancer Res*., **17**, 7294–7302.
15. Rolny,C. *et al.* (2011) HRG inhibits tumor growth and metastasis by inducing macrophage polarization and vessel normalization through downregulation of PlGF. *Cancer Cell*, **19**, 31–44.
16. Zhao,Y.M. *et al.* (2011) Validity of plasma macrophage migration inhibitory factor for diagnosis and prognosis of hepatocellular carcinoma. *Int. J. Cancer*, **129**, 2463–2472.
17. Poon,R.T. *et al.* (2002) Tumor microvessel density as a predictor of recurrence after resection of hepatocellular carcinoma: a prospective study. *J. Clin. Oncol*., **20**, 1775–1785.
18. Xiong,Y.Q. *et al.* (2009) Human hepatocellular carcinoma tumor-derived endothelial cells manifest increased angiogenesis capability and drug resistance compared with normal endothelial cells. *Clin. Cancer Res*., **15**, 4838–4846.
19. Dai,Z. *et al.* (2006) Identification and analysis of altered alpha1,6-fucosylated glycoproteins associated with hepatocellular carcinoma metastasis. *Proteomics*, **6**, 5857–5867.
20. Furuta,S. *et al.* (2006) Removal of BRCA1/CtIP/ZBRK1 repressor complex on ANG1 promoter leads to accelerated mammary tumor growth contributed by prominent vasculature. *Cancer Cell*, **10**, 13–24.
21. Zeng,Q. *et al.* (2005) Crosstalk between tumor and endothelial cells promotes tumor angiogenesis by MAPK activation of Notch signaling. *Cancer Cell*, **8**, 13–23.
22. Goffin,J.R. *et al.* (2003) Glomeruloid microvascular proliferation is associated with p53 expression, germline BRCA1 mutations and an adverse outcome following breast cancer. *Br. J. Cancer*, **89**, 1031–1034.
23. Li,L. *et al.* (2010) MicroRNA-146a and human disease. *Scand. J. Immunol*., **71**, 227–231.
24. Curtale,G. *et al.* (2010) An emerging player in the adaptive immune response: microRNA-146a is a modulator of IL-2 expression and activation-induced cell death in T lymphocytes. *Blood*, **115**, 265–273.
25. He,H. *et al.* (2005) The role of microRNA genes in papillary thyroid carcinoma. *Proc. Natl Acad. Sci. USA*, **102**, 19075–19080.
26. Bhaumik,D. *et al.* (2008) Expression of microRNA-146 suppresses NF-kappaB activity with reduction of metastatic potential in breast cancer cells. *Oncogene*, **27**, 5643–5647.
27. Hurst,D.R. *et al.* (2009) Breast cancer metastasis suppressor 1 up-regulates miR-146, which suppresses breast cancer metastasis. *Cancer Res*., **69**, 1279–1283.
28. Li,Y. *et al.* (2010) miR-146a suppresses invasion of pancreatic cancer cells. *Cancer Res*., **70**, 1486–1495.
29. Wang,X. *et al.* (2008) Aberrant expression of oncogenic and tumor-suppressive microRNAs in cervical cancer is required for cancer cell growth. *PLoS One*, **3**, e2557.
30. Ventura,A. *et al.* (2009) MicroRNAs and cancer: short RNAs go a long way. *Cell*, **136**, 586–591.
31. Zhang,T. *et al.* (2005) Overexpression of platelet-derived growth factor receptor alpha in endothelial cells of hepatocellular carcinoma associated with high metastatic potential. *Clin. Cancer Res*., **11**(24 Pt 1), 8557–8563.

Received November 21, 2012; revised April 16, 2013; accepted May 8, 2013